한국지반공학회논문집 제26권 6호 2010년 6월 pp. 21 ~ 28

The Unsaturated Stress Strain Behavior of CDG (Completely Decomposed Granite) Soils

완전 풍화된 화강풍화토의 불포화 응력-변형률 거동 특성

Ham, Tae-Gew[1] 함 태 규
Ahn, Tae-Bong[2] 안 태 봉

요 지

화강풍화토는 가장 일반적인 흙의 종류이다. 비등방성 화강풍화토의 응력-변형-강도를 측정하는 것은 사면, 옹벽, 굴착의 변형과 안정을 위하여 매우 중요하다. 불포화 강도특성을 알기 위하여 일련의 불포화 배수삼축압축시험을 시행하였다. 시험시료는 다짐방향에 각각 0, 45, 90도의 축방향각을 갖도록 하였다. 등방압축을 받는 시료의 축변형률은 다짐방향에 의하여 크게 영향을 받으며 이차압축과정에는 시간의존성은 다짐방향과 관계가 거의 없다. 삼축압축강도와 변형에 미치는 다짐방향의 영향은 저구속압과 포화토에서 더 확연한것으로 나타났다. 다짐방향과의 각도를 고려하는 불포화화강풍화토의 강도를 추정하는 방법을 제안하였다.

Abstract

Decomposed granite soil is the most common type of soils. The measurement of the stress-strain-strength behavior of anisotropic decomposed granite soils is very important for the deformation and stability analysis of slopes, retaining walls, excavations. A series of unsaturated-drained triaxial compression tests were performed to know unsaturated strength properties. The sample had three different angles of the axial (major principal) direction to the sedimentation plane (compaction plane): 0, 45 and 90 degrees. The compression strain of specimens subjected to an isotropic compression was strongly influenced by the sedimentation angle. In addition, the time dependence was independent of the sedimentation angle in relation to the deformation behavior during the secondary compression process. The effect of the sedimentation angle on the triaxial compression strength and deformation was clearly shown with low confining stress. The effect of the sedimentation angle on the compressive strength and deformation was more evident in saturated specimens. A new method of predicting the shear strength of unsaturated decomposed granite soils, considering compaction angles, was proposed.

Keywords : Anisotropy, Decomposed granite soils, Unsaturated strength, Sedimentation angle

1. Introduction

The weathering of the granite rock results in CDG (completely decomposed granite) soil in most land area. Therefore, the CDG is commonly encountered in construction field, such as riverbanks and embankments, including roads and railways, and has a stress history of compaction with their construction. In this process, the compacted

1 Member, Senior Researcher, Daewoo Engrg., Gyeonggi-DO, Korea
2 Member, Prof, Dept. of Railroad and Civil Engrg., Woosong Univ., Daejeon, Korea, tbahn@wsu.ac.kr, Corresponding Author
* 본 논문에 대한 토의를 원하는 회원은 2010년 12월 31일까지 그 내용을 학회로 보내주시기 바랍니다. 저자의 검토 내용과 함께 논문집에 게재하여 드립니다.

soil possesses an anisotropic property. Much laboratory work has been conducted to find the compressibility or mechanical properties of compacted materials. For compacted specimens employed in conventional triaxial tests, the direction of the compaction loading corresponded with the direction of the major principle stress. However, the stress conditions in a soil structure caused by additional loading, such as an earthquake, should vary in terms of the direction of the major principal stress. Therefore, in order to study stability and deformability of a structure using compacted materials, it is necessary to understand the anisotropic properties for the unsaturated compacted material. Although it has been widely recognized, studies of the anisotropic property of compacted materials have been limited to clayey soils (Livneh and Komornik, 1967; Onitsuka and Hayashi, 1979). Conversely, saturated clay and soil have been studied by many researchers (Oda et al., 1978; Tatsuoka et al., 1990), but previous researches concerning anisotropic property of CDG materials are limited. Therefore, it is necessary to collect substantial data in order to understand the mechanical properties of CDG soils.

A series of unsaturated-drained triaxial compression tests were performed on unsaturated compacted materials. The tests were planned to find not only the degree of anisotropy for the sedimentation angle of the compacted material, but also the influences of the confining stress, degree of saturation and specimen preparation method on the anisotropic properties. The test results show not only the degree of anisotropy considering the sedimentation angle of the compacted material, but also the influence on the unsaturated CDG materials.

2. Experiments

2.1 Material Properties

The physical properties of the sample are shown in Table 1, and the grain size distribution curve of the materials in Fig. 1. U_c is the coefficient of uniformity, and the degree of weathering was determined from ignition loss. Quartz, feldspar, and colored mineral contents of this sample were about 23, 62 and 15%, respectively. Ignition loss of Toyoura sand, mostly composed of quartz, with a small degree of weathering, was 0.4. The ignition loss of the sample was 1.83.

2.2 Method

Decomposed granite soil with optimum moisture content (w = 13%) was compacted in a container (200 mm×100 mm×200 mm) by hitting with a 19.6N rammer. The density of the compacted materials was controlled by the relative compaction, R, to be 90%. The relative compaction was defined as the percentage of the density to the maximum dry density obtained from each compaction test. The soils are compacted by 1.8 cm at each layer to make 20 cm height. The rectangular sample was frozen at under -20℃ followed by cylindrical triaxial compression of the specimens into a 50 mm diameter and 100 mm height using a core bit machine, as shown in Fig. 2. The liquefied nitrogen was sprinkled to the sample with 80 kPa to avoid disturbance. The sample had three different angles of the axial (major principal) direction to the sedimentation plane

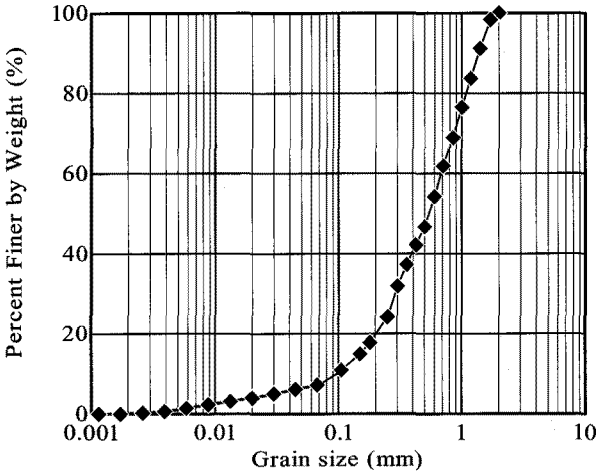

Fig. 1. Grain size distribution curve

Table 1. Physical properties of soils used

Sample	Max. Grain size (mm)	G_s	Ignition loss (%)	U_c	w_{opt}	ρ_{max} (g/cm^3)
Shimonoseki	< 2	2.68	1.83	7.14	13.24	1.78

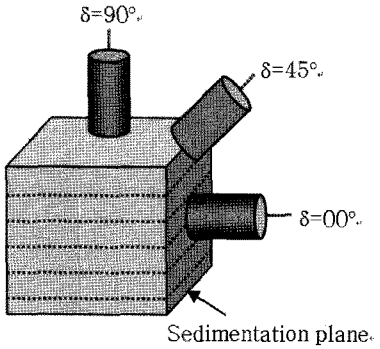

Fig. 2. Schematic diagram of showing angles of axial direction δ with respect to the bedding plane

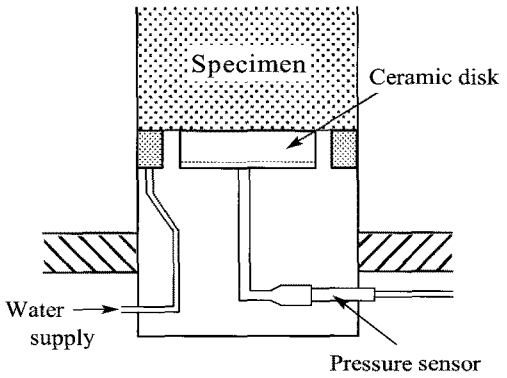

Fig. 3. Schematic diagram of triaxial type discharge capacity test device

(compaction plane): 0, 45 and 90 degrees.

Specimens were set up under a 20 kPa confining pressure, with melting for about 6-hours. After this, confining pressures up to, 30, 60, 120 or 240 kPa were applied for 1 or 10 hours, in order to find the time dependency of the mechanical behavior of the unsaturated compacted materials.

Also, a series of suction tests were performed to investigate the suction of unsaturated CDG soils. Tests were carried out on two sets of specimens. The first set of specimens was similar to the frozen specimens used in the triaxial tests. For comparison purposes, the second set of specimens consisted of compacted soils having different initial degrees of saturation, S_r, ranging from 40-90%.

2.3 Suction Test

The suction test was equipped with a ceramic disk with an air entry value (AEV) of 270 kPa as shown in Fig. 3. It is worthy of mentioning that the frozen specimens thawed after about 8 hours, after which suction was measured. The influence of suction on strength parameters was estimated from water contents of unsaturated samples.

The drained triaxial compression tests were carried out on both unsaturated (S_r = 60%) and saturated specimens at a constant strain rate of 0.1 mm/min. The triaxial apparatus was equipped with a double cell to measure the volume change of the unsaturated specimens. The volume change of saturated specimens was measured by a burette. At small strain levels (during consolidation and initial part of shearing), the axial strain was measured by a gap sensor which can measure ε_a up to 2.0%, while at higher strain levels, an axial displacement transducer was employed.

Fig. 4 shows the relationship between the degree of saturation and the initial suction for the unsaturated specimens. As expected, suction rapidly decreased as the degree of the saturation increased. Moreover, it can be observed that there is not much difference in the water retention characteristics of frozen and unfrozen samples. Furthermore, the angle appears not to have significant effect on the soil water characteristic curve.

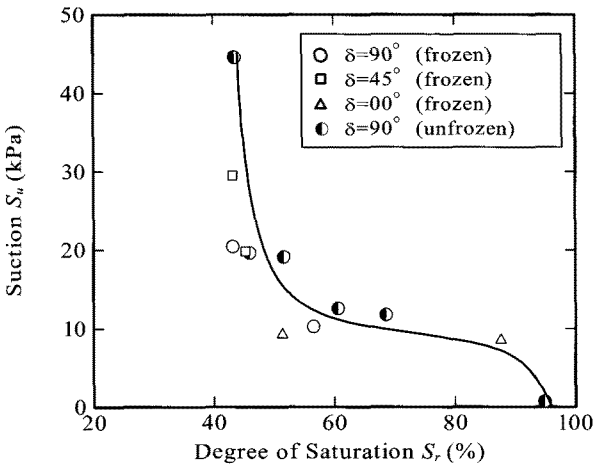

Fig. 4. Relationship between suction and degree of saturation

3. Experimental Results

3.1 The Effect of the Sedimentation Angle on the Compression Settlement

Fig. 5 shows the relationship between the elapsed com-

pression time and the axial strain for a sample subjected to a 60 kPa confining stress. There were two compression processes: one was the primary compression process from the beginning to the end of the confining pressure loading, and the other the secondary compression process after the end of the confining pressure loading. The amounts of axial strain during the primary and secondary compressions were referred to as S_1 and S_2, respectively, as shown in Fig. 5.

The isotropic compression behavior, S_1, increased suddenly due to the immediate settlement during the primary compression process, after then S_2 showed only a slight non-linear relationship with the function of the logarithm of time during the secondary compression process.

Fig. 6 shows the relationship between the axial strain and time under the conditions of 60 kPa of confining pressure and 10 hours compressive stress. The arrow in the Fig. 6 represents the moment the load ended. As δ of the specimen decreased from 90° to 0°, the axial strain S_1 increased.

Fig. 7 shows the effect of the confining pressure on the relationship between the axial strain and the duration of compressive stress for samples subjected to 30, 60, 120, 240 kPa confining pressures for specimens with δ = 90°. As the confining stress increased, the amount of axial strain S_1 also increased. The arrows in the Fig. 7 represent the moment the load ended. Then, the amount of axial strain, S_2, was approximately the same for all confining stresses. The behavior of deformation during the secondary compression process was verified as not having any dependency on the confining stress. S_2 was considered to be related to the particle rearrangement and decreased suction factors that were the result of the compression.

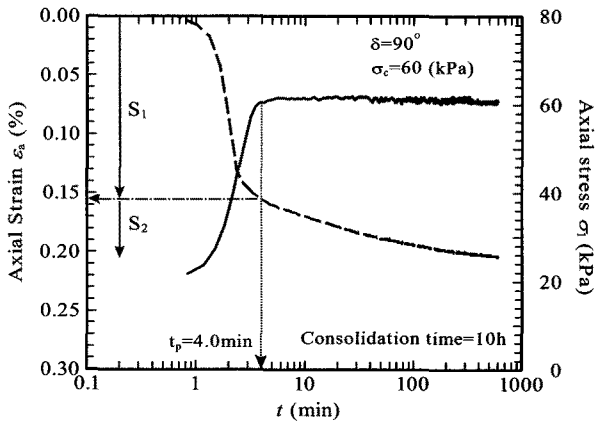

Fig. 5. Relationship between axial strain, axial load and time of compression (δ=90°)

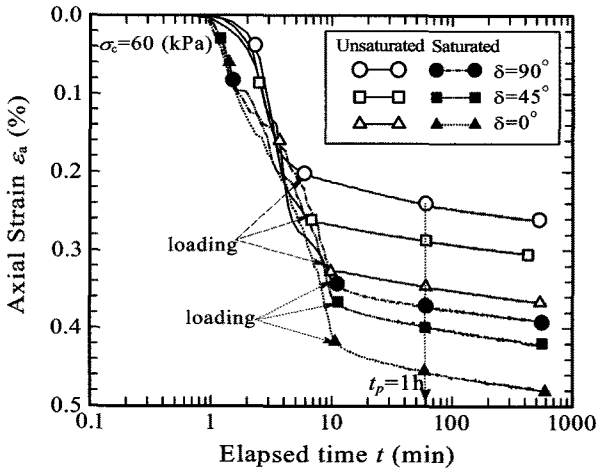

Fig. 6. Relationship between axial strain and time of compression

3.2 The Effect of the Sedimentation Angle on the Strength

In order to investigate the shear property of the compacted specimen with 90, 45 and 0 degree sedimentation angles, drained triaxial compression tests were performed. The deviator stress-axial strain and axial-volumetric strains diagrams for the specimen compressed at 120 kPa are shown in Fig. 8.

The deviator stress showed a clear maximum stress points, which then slowly decreased as shown in Fig. 8. As the value of δ increased from 0° to 90°, the maximum value of the deviator stress q_{max} also increased, but the

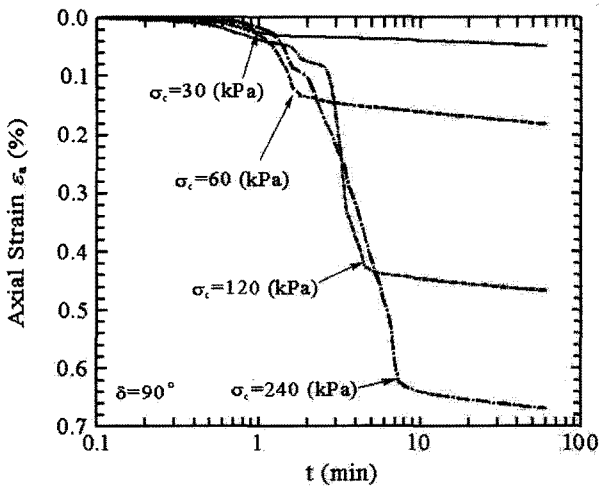

Fig. 7. Relationship between Axial strain and compression time (min)

axial strain at q_{max} decreased. In addition, the dilatancy rate at the point of failure increased with increasing δ. Fig. 9 shows the change in the deviator stress obtained for strains up to 0.05% for the specimens.

As the value of δ increased from 0° to 90° the angle (ϕ_{peak}) also increased as shown in Fig. 10. The angle (ϕ_{peak}) of the 10 hours compressed specimens appeared to be approximately 2 degrees lower than that of the 1-hour compressed specimens. The degrees of saturation of the 1 and 10 hours compressed specimens were approximately 60 and 65%, respectively. Thus, the decrease in the strength over 10 hours would be related to the increase in saturation of the specimen, which also caused the decrease in suction.

Fig. 11 shows the relationship among cohesion c, the internal friction angle ϕ and the angle δ, for both unsaturated and saturated specimens. These data were obtained by applying the Mohr-Coulomb failure criterion to the results of the triaxial compression tests. Both saturated and unsaturated specimens showed similar tendencies with respect to friction angle, i.e., as the δ value decreased from 90° to 0°, the internal friction angle also decreased. In contrast, cohesion increased as δ increased for unsa-

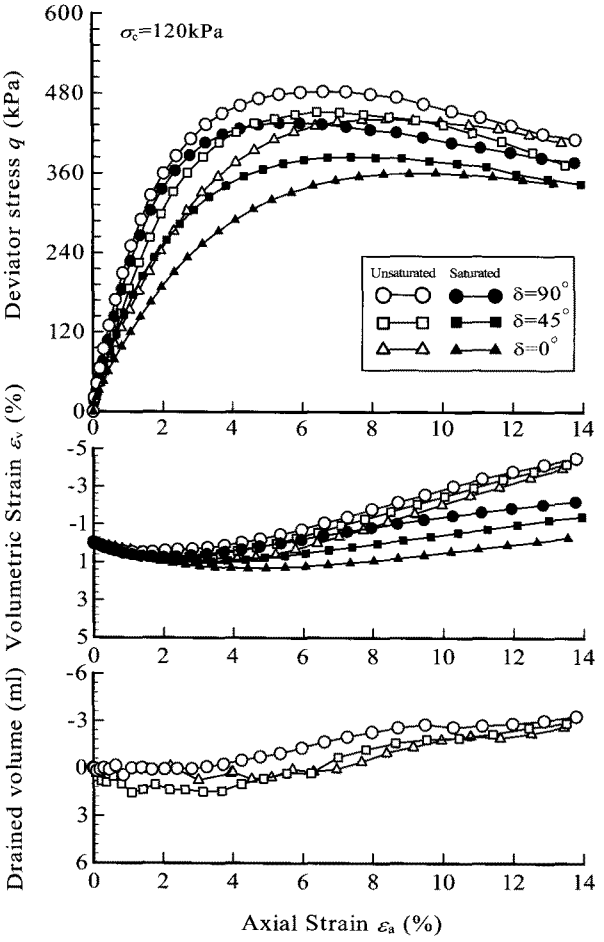

Fig. 8. Relationship between axial strain and deviator strain, volumetric strain and drain volumetric strain

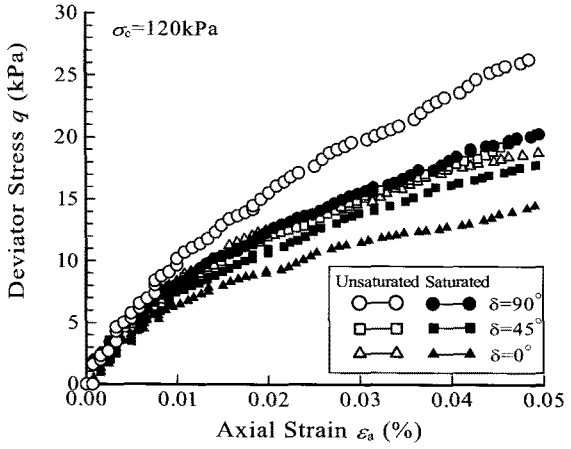

Fig. 9. Stress- strain relations (up to ε_a=0.05%)

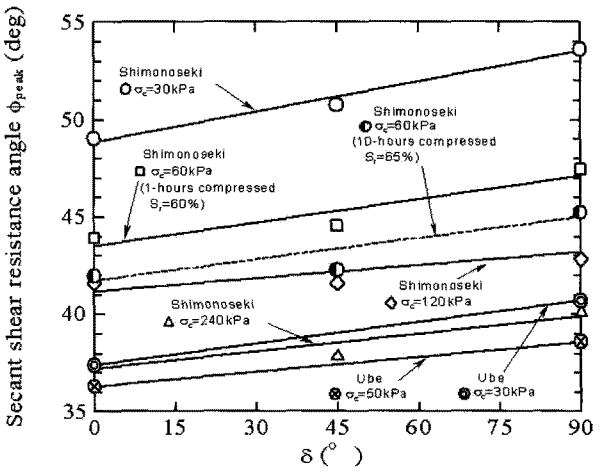

Fig. 10. Relationship between secant shear resistance angles at peak shear stress and δ

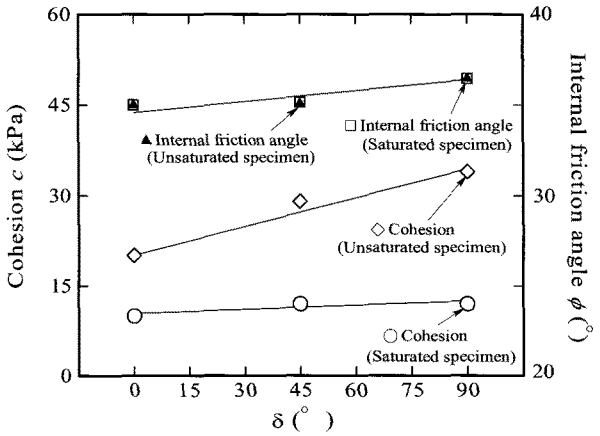

Fig. 11. Relationship among cohesion, internal friction angle and δ

turated specimen due to suction, but for saturated specimen, δ seemed to have no effect. The increased cohesion due to suction in unsaturated samples can be expressed apparent cohesion. Thus, it can be surmised that compacted specimens have anisotropic mechanical properties with respect to cohesion due to the presence of suction.

Based on the results of the unsaturated and saturated drained triaxial compression tests on compacted decomposed granite soils, it can be concluded that the effect of the angle between loading and bedding plane (i.e., δ) on the strength was more significant in unsaturated specimen than in saturated specimen.

Fig. 12 shows the relationship between the secant shear resistance angles at peak shear stress (ϕ_{peak}) and the mean principal stress, p. As the mean principal stress increased, ϕ_{peak} decreased steeply. The slope became steeper as δ became large. The effect of the sedimentation angle on the strength of deformation was clear with low mean principal stress. In the case of Ube, the tendency for a steep slope was shown to be very gentle with increases in the mean principal stress, p, compared with the data of Shimonoseki. It was thought that the initial fabric arrangement would remain nearly constant in a low confining stress. As the confining stress increased, the particles were rearranged by particle breakage, and the effect of the sedimentation angle disappeared under high confining stress.

3.3 The Effect of the Sedimentation Angle on the Dilatancy

In order to show the effect of the sedimentation angle on the dilatancy, the ratio of the volumetric strain increment to the increment of the axial strain at peak stress conditions, $(-d\varepsilon_v/d\gamma)_{peak}$, was examined. Fig. 13 shows the ratio of $(-d\varepsilon_v/d\gamma)_{peak}$ for an angle of sedimentation to $(-d\varepsilon_v/d\gamma)_{peak}$ for a δ of 90°. The ratio $(-d\varepsilon_v/\varepsilon\gamma)_{peak}$ / $(-d\varepsilon_v/\varepsilon\gamma)_{peak}$ at = 90° was plotted against δ. As the confining stress increased, the ratio, $(-d\varepsilon_v/d\gamma)_{peak}$ / $\{(-d\varepsilon_v/d\gamma)_{peak}$ at $\delta = 90°\}$ decreased. The $(-d\varepsilon_v/d\gamma)_{peak}$ / $\{(-d\varepsilon_v/d\gamma)_{peak}$ at $\delta = 90°\}$ with a confining stress of 30 kPa was 0.58. As the confining stress increased, the value of $(-d\varepsilon_v/d\gamma)_{peak}$ / $\{(-d\varepsilon_v/d\gamma)_{peak}$ at $\delta = 90°)\}$ was approximately 1.0.

The CDG soils had lower values of $\{(-d\varepsilon_v/d\gamma)_{peak}$ at $\delta = 0°\}$/$\{(-d\varepsilon_v/\varepsilon\gamma)_{peak}$ at $\delta = 90°\}$ than the data for the air pluviated decomposed granite and Toyoura sand.

Fig. 14 shows the relationship between the increment of strength due to dilatancy, $\phi_{peak} - \phi_{cv}$, and the dilatancy rate, $(d\varepsilon_v/d\gamma)_{peak}$ at failure. As $(d\varepsilon_v/d\gamma)_{peak}$ increased, $\phi_{peak} - \phi_{cv}$ also increased. The same tendency was obtained for all specimens used in this paper. It was also recognized that although the sedimentation angle and preparation methods were different, the increment of strength was related to the dilatancy rate at failure. Therefore, it can be concluded that the difference between the peak strength ϕ_{peak} and the residual strength ϕ_{cv} was dominated by the dilatancy for compacted specimens.

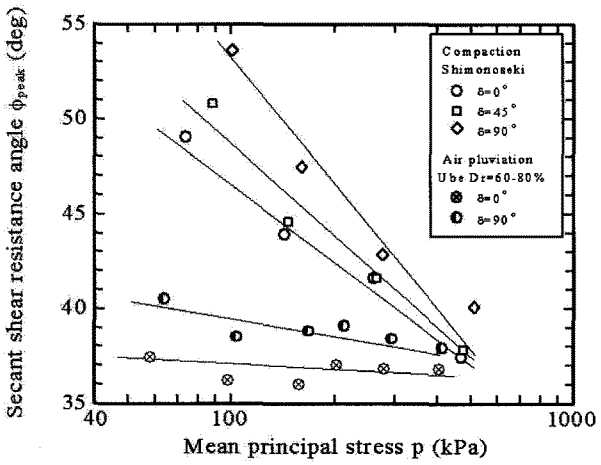

Fig. 12. Relationship between secant shear resistance angles at peak shear stress and mean principal stress

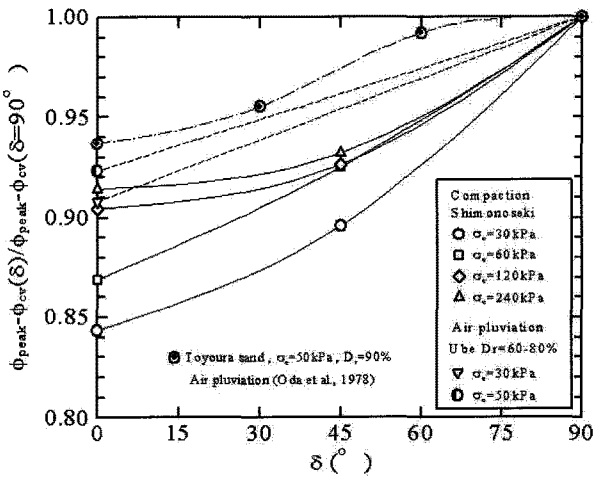

Fig. 13. $\{(-d\varepsilon_v/d\gamma)_{peak}(\delta)\}/\{(-d\varepsilon_v/d\gamma)_{peak}$ for a δ of 90°}

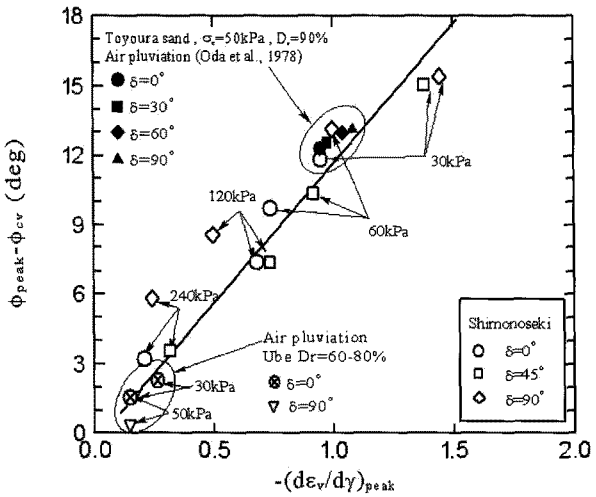

Fig. 14. Relationship between $(\phi_{peak} - \phi_{cv})$ and $-(d\varepsilon_v / d\gamma)$

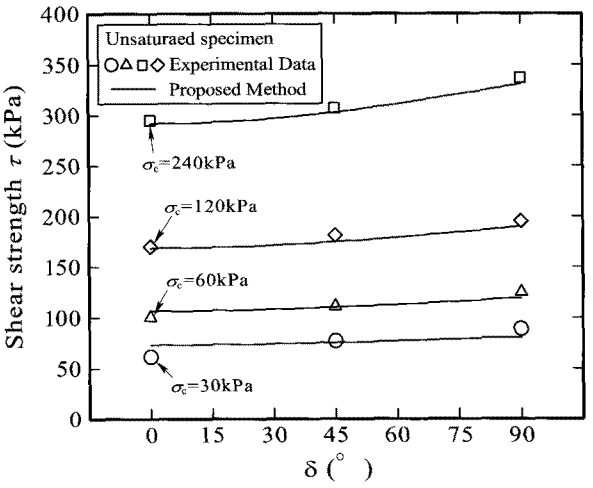

Fig. 15. Relationship between shear strength and angle δ

4. Proposed Prediction Method of Unsaturated CDG Soils

Based on the results obtained, a new procedure is proposed to determine the value of internal friction angle ϕ to be used for estimating the shear strength τ of an unsaturated compacted specimen. In the following, ϕ is obtained considering the angle of axial loading (direction of maximum principal stress) with respect to bedding/ compacted plane, δ. The internal friction angle $\phi(\delta)$ at each orientation can be calculated by using Eq. (1).

$$\phi(\delta) = \phi(\delta = 90^\circ) \times (1 - \alpha \cos\delta) \tag{1}$$

where $\phi(\delta = 90°)$ is the internal friction angle of saturated specimen when $\delta = 90°$, and α is an empirical parameter that varies with the type of soil or degree of compaction. α varies with soils and compaction degree. In this study, α is 0.08, and Nakata et al. (1998) showed 0.08 on Ube granite soil and Toyiura sand.

Next, the shear strength τ of the saturated specimen for any angle δ is calculated by using Eq. (2).

$$\tau(\delta) = c(\delta = 90^\circ) + (\sigma - u_w)\tan\phi(\delta) \tag{2}$$

where $c(\delta = 90°)$ is the cohesion of a saturated specimen at $\delta = 90°$ obtained from experiments, σ is the total stress and u_w is the pore water pressure.

Bishop (1960) proposed the effective stress of unsaturated soil as shown in Eq. (3).

$$\sigma' = (\sigma - u_a) + \chi(u_a - u_w) \tag{3}$$

where σ' is the effective stress, u_a is the pore air pressure and χ is a constitutive material property that depends on degree of saturation. In this study, χ was calculated by using Bishop's method (1960). The results were as follows: for $\delta = 0°$, $\chi = 0.78$; for $\delta = 45°$, $\chi = 0.75$; and for $\delta = 90°$, $\chi = 0.79$. The results indicate that the effect of δ on χ is negligible.

Finally, the shear strength τ of the unsaturated specimen for each value of δ can be calculated by using the following equation:

$$\tau(\delta) = c(\delta = 90^\circ) + \{(\sigma - u_a) + \chi(u_a - u_w)\}\tan\phi(\delta) \tag{4}$$

$$\tau(\delta) = c(\delta = 90^\circ) + \chi(u_a - u_w)\tan\phi(\delta) + (\sigma - u_a)\tan\phi(\delta) \tag{5}$$

The term of $\chi(u_a - u_w)\tan\phi(\delta)$ in equation (5) is apparent cohesion caused by suction on unsaturated samples. Apparent cohesion also increases with δ.

Fig. 15 shows the curves representing the relationship between the shear strength and δ of unsaturated specimens, as given by Eq. (4). Moreover, the data points indicated in Fig. 15 are the measured values from tests on unsaturated specimen. It can be observed that a good agreement exists between the proposed and measured values. Thus, it can be surmised that the dependency of the shear strength of the unsaturated specimen on δ is caused mainly

by the dependency of internal friction angle on δ.

5. Conclusions

This paper introduces a series of unsaturated-drained triaxial compression tests which were performed on CDG (completely decomposed granite) materials. Typical test results from a series of triaxial tests for unsaturated samples were planned to find the effect of not only sedimentation angle, but the influence of confining stress, degree of saturation and specimen preparation method on the anisotropic properties. Also, a new prediction method is proposed for unsaturated CDG soils depending sedimentation angles. Following conclusions may be drawn.

(1) The compression strains of specimens were strongly influenced by the sedimentation angle.
(2) The Secant Young's modulus showed the same behavior for all specimens, even with different δ.
(3) The effects of the sedimentation angle on the triaxial compression strength and deformation were clear with a low confining stress.
(4) The difference between the peak strength ϕ_{peak} and the residual strength ϕ_{cv} was dominated by the dilatancy for compacted specimens.
(5) The compacted specimen can be considered to have anisotropic mechanical properties, the same as the initial fabric anisotropy of sand.
(6) A procedure is proposed to estimate the shear strength τ of unsaturated compacted specimen taking into account the angle δ.

References

1. Hardin, B.O. and Richart, F. (1963), "Elastic wave velocities in granular soils", *Journal of Soil Mechanics and Foundation Division*, ASCE, Vol.89, No.SM1, pp.33-65.
2. Hardin, B.O. and Black, W. L. (1969), "Vibration modulus of normally consolidated clay", *Journal of the SMF Div., Proc. ASCE*, Vol.95, No.SM6, pp.1531-1537.
3. Kohata. et al. (1995), "Inherent and induced anisotropy of sedimentary softrock", *Proc. Of 10ARC*, pp.33-36.
4. Livneh, M. and Komornik, A. (1967), "Anisotropic strength of compacted clay", *Proc., 3rd ASIAN Reg. Conf. On SMFE*, Vol.1, pp.298-304.
5. Lambe, T. W. (1958), "The structure of compacted clay", *Proc., Journal of the Soil Mechanics and Foundation Division, ASCE*, Vol.84, No.SM2, paper 1654.
6. Nakata, Y., Hyodo, M. and Murata, H. (1998), "Single particle crushing and mechanical behavior of decomposed granite soil", *Proceedings of the international symposium on problematic soils, IS-TOHOKU'98. SENDAI, JAPAN*: pp.483-497.
7. Oda, M., Koishikawa, I., and Higuchi, T. (1978), "Experimental study of anisotropic shear strength of sand by plane strain test", *Soils and Foundation*, Vol.18, No.1, pp.25-38.
8. Onitsuka, K. and Hayashi, S. (1979), "Studies on compression and strength Anisotropy of compacted soils", *in Japanese. JSCE.* Vol.19, No.3, Sept, pp.113-123.
9. Seed, H. B., Mitchell, J.K. and Chan, C.K. (1960), "The strength of compacted cohesive soils", *ASCE., Research Conf. On the Shear Strength of Cohesive Soil, Boulder*, Colorado, pp.169-273.
10. Shibuya, S., Mitachi, T., Fukuda, F. and Degoshi, T. (1995), "Strain rate effects on shear modulus and damping of normally consolidated clay", *Geotechnical Testing Journal*, Vol.18, No.3, pp.365-375.
11. Tatsuoka, F., Nakamura, S., Huang, C. and Tani, K. (1990), "Strength anisotropy and shear band direction", *Soils and Foundation*, Vol.30, No.1, pp.35-54.
12. Tatsuoka, F. amd Shibuya, S. (1992), "Deformation characteristics of soils and rocks from field and laboratory tests", *Keynote Lecture, Proc. of 9th Asian Regional Conf. on SMFE*, Vol.2, pp.101-170.

(접수일자 2010. 3. 9, 심사완료일 2010. 6. 20)

Notation

c - cohesion (kPa)
D_c - degree of compaction (%)
E_{sec} - secant modulus at ε_a = 0.001% (kPa)
p - mean principal stress (= $[\sigma_1 + 2\sigma_3]/3$) (kPa)
q - axial deviator stress (= $\sigma_1 - \sigma_3$) (kPa)
S_r - degree of saturation (%)
S_1 - axial strain after primary consolidation (%)
S_2 - axial strain after secondary consolidation (%)
t_p - time to end of primary consolidation (min)
α - an empirical parameter for calculating friction angle
ε_a - axial strain (%)
ε_v - volumetric strain (%)
σ_1 - maximum principal stress (kPa)
σ_3 - minimum principal stress (kPa)
ϕ - internal friction angle (°)
χ - a constitutive material property that depends on degree of saturation
δ - angle between the major principal axis direction and the bedding plane (°)
U_c - coefficient of uniformity